Saturn-ring proton backlighters for the National Ignition Facility

A. B. Zylstra (iD), R. S. Craxton (iD), J. R. Rygg (iD), C.-K. Li, L. Carlson, M. J.-E. Manuel, E. L. Alfonso, M. Mauldin, L. Gonzalez, K. Youngblood (iD), E. M. Garcia, L. T. Browning, S. Le Pape, N. Candeias Lemos (iD), B. Lahmann (iD), M. Gatu Johnson (iD), H. Sio, and N. Kabadi

View Online   Export Citation   CrossMark

Saturn-ring proton backlighters for the National Ignition Facility

View Online   Export Citation   CrossMark

A. B. Zylstra,[1,a] 🔟 R. S. Craxton,[2] 🔟 J. R. Rygg,[2] 🔟 C.-K. Li,[3] L. Carlson,[4] M. J.-E. Manuel,[4] E. L. Alfonso,[4]
M. Mauldin,[4] L. Gonzalez,[4] K. Youngblood,[1] 🔟 E. M. Garcia,[2] L. T. Browning,[2] S. Le Pape,[1]
N. Candeias Lemos,[1] 🔟 B. Lahmann,[3] 🔟 M. Gatu Johnson,[3] 🔟 H. Sio,[1] and N. Kabadi[3]

AFFILIATIONS

[1] Lawrence Livermore National Laboratory, Livermore, California 94550, USA
[2] Laboratory for Laser Energetics, University of Rochester, Rochester, New York 14623, USA
[3] Plasma Science and Fusion Center, Massachusetts Institute of Technology, Cambridge, Massachusetts 02139, USA
[4] General Atomics, San Diego, California 92121, USA

[a] Author to whom correspondence should be addressed: zylstra1@llnl.gov

ABSTRACT

Proton radiography is a well-established technique for measuring electromagnetic fields in high-energy-density plasmas. Fusion reactions producing monoenergetic particles, such as D^3He, are commonly used as a source, produced by a capsule implosion. Using smaller capsules for radiography applications is advantageous as the source size decreases, but on the National Ignition Facility (NIF), this can introduce complications from increasing blow-by light, since the phase plate focal spot size is much larger than the capsules. We report a demonstration of backlighter targets where a "Saturn" ring is placed around the capsule to block this light. The nuclear performance of the backlighters is unperturbed by the addition of a ring. We also test a ring with an equatorial cutout, which severely affects the proton emission and is not viable for radiography applications. These results demonstrate the general viability of Saturn ring backlighter targets for use on the NIF.

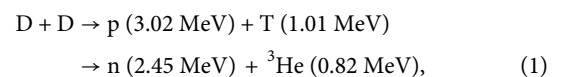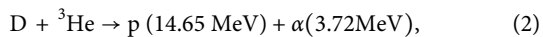Published under license by AIP Publishing. https://doi.org/10.1063/5.0021027

I. INTRODUCTION

High-energy-density plasmas (HEDPs) have electromagnetic fields, which can be self-generated by mechanisms such as the Biermann battery,[1,2] imposed by an external source such as a solenoid-generated magnetic field,[3] or generated by currents as in a Z-pinch experiment. Understanding the field generation and evolution is important for our fundamental understanding of HEDP and has relevance to the pursuit of inertial confinement fusion, as self-generated or applied magnetic fields may affect transport mechanisms such as thermal conductivity. Electromagnetic fields are also present in HEDP used for scaled laboratory astrophysics experiments and thus have relevance to several astrophysical phenomena.

Diagnosing electromagnetic fields in HEDP is challenging. Typically, radiographic measurements are performed using charged-particle deflectometry, where the electromagnetic fields are inferred by the charged-particle deflection due to the Lorentz force [$\vec{F} = q(\vec{E} + \vec{v} \times \vec{B})$]. Techniques for performing deflectometry have been developed with proton sources as a backlighter using high-intensity lasers to accelerate ions via the target-normal sheath acceleration mechanism[4–7] or using a shock-driven "exploding pusher" implosion to generate fusion-reaction products.[8,9] These techniques have been highly successful in studying electromagnetic fields produced by direct-drive implosions,[10,11] by indirect-drive implosions,[12,13] during magnetic reconnection,[14–16] self-generated by the Rayleigh–Taylor instability,[17,18] by the Weibel instability,[19] around scaled astrophysical jets,[20] and in the turbulent dynamo.[21]

At present, proton backlighting on the National Ignition Facility (NIF) is performed using the implosion technique. NIF backlighters have been demonstrated using 860 μm diameter thin-glass capsules containing D^3He fuel,[22] which are driven by 6–8 of the 48 NIF quads. These capsules produce the fusion reactions,

$$D + D \rightarrow p\,(3.02\ \text{MeV}) + T\,(1.01\ \text{MeV})$$
$$\rightarrow n\,(2.45\ \text{MeV}) + {}^3He\,(0.82\ \text{MeV}), \quad (1)$$

$$D + {}^3He \rightarrow p\,(14.65\ \text{MeV}) + \alpha(3.72\text{MeV}), \qquad (2)$$

with ~10^{10} protons produced by each reaction and emitted isotropically from an 80 μm full-width at half-maximum (FWHM) source. More recent work has used smaller capsules (~430 μm diameter),[23] which are advantageous because they have a smaller source size and thus an effectively higher resolution.

The NIF presents several unique challenges to using such small capsules. Since removing the 2ω continuous phase plates[24] from the backlighter quads would be a prohibitive time cost, given typical allocations of experimental time on the facility, they must be used, resulting in a focal spot (~1 mm) that is significantly larger than the backlighter capsule diameter. This results in reduced energy coupling to the target and a large amount of "blow-by" energy, which can potentially affect the physics target to be radiographed, depending on the geometry, and could represent a danger to the laser system, in particular, the final (LM8) mirror in the infrared portion of the laser.[24] The blow-by can constrain the laser configuration: in prior experiments, either a small number of beams was used at high power, but with opposing quads within ~20° shuttered, or the backlighter is driven with a much larger number of drive beams at low power. Most campaigns to date use a design with 16–20 quads used to drive the backlighter at low power, a significant fraction of the total NIF, which has 48 quads divided into four angular "cones" in the upper and lower hemispheres at 23.5, 30, 44.5, and 50° from the axis. Furthermore, because of these geometric constraints (the beam locations make driving the capsule equator difficult) and the need to simultaneously drive the subject target, experiments requiring many quads to irradiate the backlighter often have a significantly asymmetric backlighter drive, leading to reduced performance (sensitivity to illumination nonuniformities has been demonstrated[25]). It is preferable to drive the backlighter with fewer beams, at higher power per beam, but better symmetry. Mitigating these limitations would significantly broaden the capabilities for proton backlighting on the NIF.

In this paper, we present a novel backlighter concept utilizing a "Saturn" ring, thereby enabling the use of small backlighter capsules with mitigated blow-by light, enabling higher-resolution probing of HEDP experiments with additional flexibility on the experimental configuration. The nuclear performance of these targets is shown to be identical to those without the ring. Some evidence of electromagnetic fields that develop around the ring is observed, leading us to conclude that proton probing orthogonal to the plane of the ring is feasible, but using a cutout in the ring is not viable for extending the applicability of the target for measurements in the plane of the ring.

This paper is organized as follows: the design of the Saturn ring backlighter is presented in Sec. II, the experimental demonstration and interpretation are given in Sec. III, and this paper is concluded in Sec. IV.

II. SATURN RING DESIGN

The "Saturn" target is a concept in which a plastic ring is placed around the equator of the capsule. The concept has been tested on OMEGA[26,27] and proposed as a polar-drive ignition scheme for the NIF.[28] In the latter, the main benefit of the Saturn target is that refraction in the plasma ablated around the ring enhances drive on the equator of the capsule, improving uniformity. For proton backlighting, the ring can also be used to absorb the outer regions of the beam spot, dramatically reducing the amount of blow-by laser energy. The enhanced uniformity on the capsule and improved coupling are also beneficial.

Saturn targets have been fabricated and shot at OMEGA, and targets at a comparable scale would be used on the NIF. The capsule can be mounted within the ring by tent or stalk. These shock-driven implosions are low convergence (~4) and are not sensitive to engineering features. The capsules are diffusion filled, so a fill tube is not required.

Design calculations have been performed using the 2-D radiation-hydrodynamics code SAGE.[29] In the simulations, eight NIF quads drive the capsule using ~50 kJ of energy in a 900 ps square pulse (to approximate the experimental pulse, the power increases linearly to the 2.2 TW/beam at 280 ps and then falls to zero linearly from 800 ps to 900 ps). Four quads from the top and bottom of any single ring angle (23.5°, 30°, 44.5°, or 50°) could be used; for this work, we use 44.5° quads. An example simulation is shown in Fig. 1 illustrating the key physics. Laser rays are traced through the target, with a 440 μm diameter capsule, early in the drive (100 ps, left) and approximately halfway through (400 ps, right). At early time, most rays are absorbed or reflected by the capsule or ring, but a few pass through the gap (only the two brown rays in Fig. 1 pass through undeflected). As the capsule and ring ablate, the overall absorption improves, and refraction enhances the equatorial drive on the capsule.

The primary design parameter for the Saturn target is the inner diameter of the encircling ring. If the inner diameter is too small, the drive uniformity is compromised, while if the ring is too large, there is significant blow-by light through the gap. An optimization study is shown in Fig. 2, which plots the drive uniformity and scattered
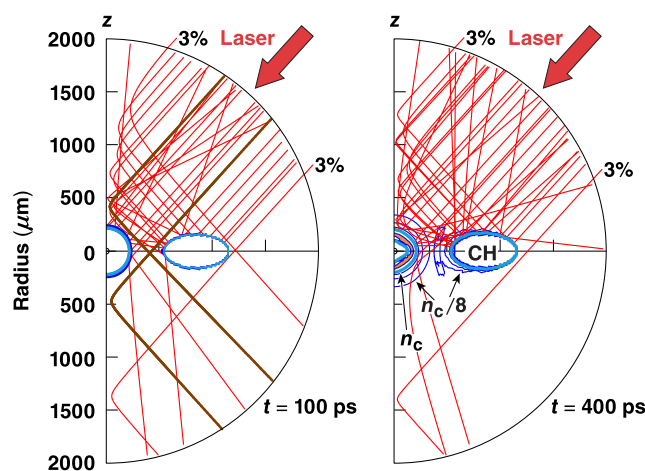

FIG. 1. SAGE calculations of a Saturn backlighter target, showing electron density contours and laser rays traced through the target at early time (100 ps into the drive, left) and halfway through (400 ps, right). The hydrodynamic profiles are rotationally symmetric about the vertical (z) axis. The extreme rays modeled have intensity 3% of the maximum.
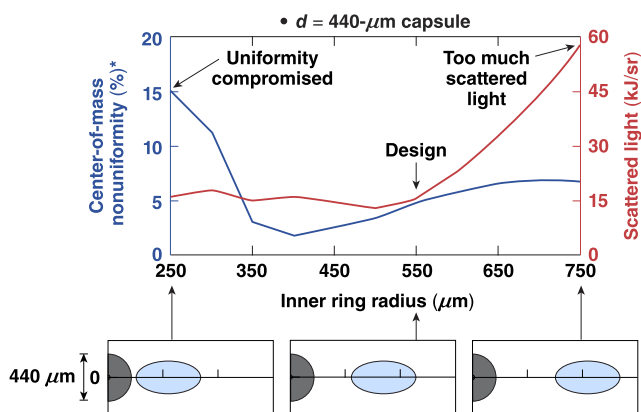
FIG. 2. Drive uniformity at 400 ps (blue curve, left axis) and scattered light flux (red curve, right) vs Saturn ring inner radius. The target dimensions with a 440 μm capsule are shown to scale at the bottom. The ring cross section is 600 μm wide and 300 μm high.

FIG. 4. Scattered light fluence and flux on the final optics mirror vs full-angle opening in the ring for the worst-case cone for illumination (23.5°). Up to 0.07 J/cm^2 on the final mirror is safe.

light flux as a function of the inner ring radius. The drive uniformity is defined here as the uniformity of the center-of-mass radius of the imploding shell at 400 ps, evaluated over the full 4π solid angle. For the scattered light flux, all the individual NIF beams are ray traced in 3D, and the maximum flux in any direction is used. The simulations predict that good drive uniformity is achieved for inner radii between 350 μm and 550 μm, while the scattered (blow-by) light is optimal for any inner radii 550 μm or less. The design is thus 550 μm. This has the additional advantage that a single ring size can accommodate both small (440 μm diameter) and large (860 μm diameter) capsules. A similar result was obtained in Ref. 30 for a ring with a triangular cross section. Figure 3 shows the density contours and laser ray traces approximately halfway through the drive for both the small (left) and large (right) capsules within the same Saturn ring. The gap between the large capsule and the ring is (just)
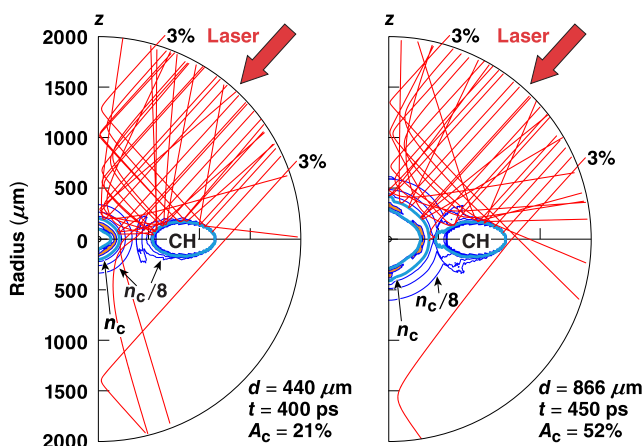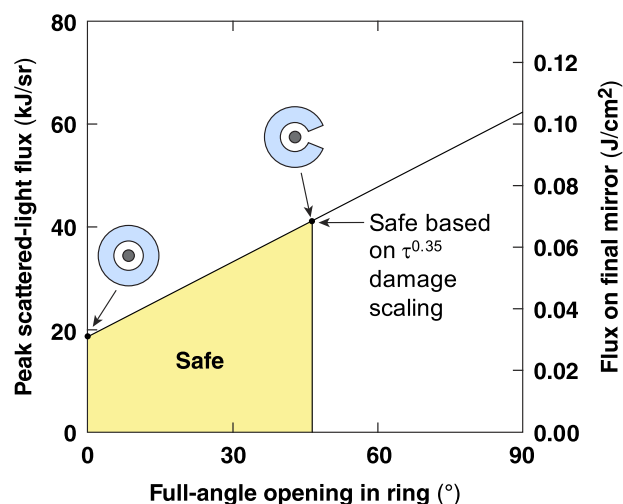
sufficient to avoid compromising the capsule implosion uniformity. The time-integrated absorption into the capsule (A_c) is significantly higher for the larger target (52% compared with 21%).

For the 440 μm diameter capsule, the SAGE calculations predict that using the Saturn ring reduces the maximum scattered light fluence by nearly an order of magnitude, from 174 kJ/sr to 19 kJ/sr, even for the worst-case illumination cone (23°). This corresponds to ~0.03 J/cm^2 on the final optics, a very safe level. While the Saturn target is naturally oriented for radiography in the direction orthogonal to the ring, radiography in the ring's plane is also possible using a partial opening in the ring. Simulations indicate that a full-opening angle of ~45° is possible with acceptable levels of blow-by light, which is shown in Fig. 4. Figure 4 takes into account the 0.35-power scaling of damage fluence with pulse width τ.[31] The maximum safe flux on the final mirror shown as ~0.069 J/cm^2 scales to $0.069 \times (3.0/0.9)^{0.35} = 0.105$ J/cm^2 at 3 ns, the predicted flux[32] for NIF shots N150702-001 and N150702-004, both of which were safely shot using a 3-ns ramp pulse.

III. EXPERIMENTAL DEMONSTRATION

In this work, we focused on an experimental demonstration using small (440 μm diameter) glass exploding pusher capsules. For the Saturn ring, we used a design with an inner diameter of 0.7 mm and an elliptical cross section with major diameter in the plane of the ring of 0.6 mm and a minor diameter (height) of 0.3 mm. A cutaway with actual (nominal) dimensions of a ring, made of plastic, is shown in Fig. 5.

We report on a series of three shots: a backlighter capsule without any ring (N151214-001), a full ring (N180925-003), and a ring with a 30° cutaway toward Diagnostic Instrument Manipulator (DIM)[38] 90-78 (N180925-004). The targets used for these shots are shown in Fig. 6. The capsules used are all 440 μm in diameter, with
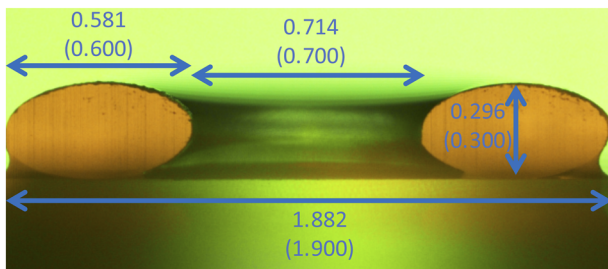

FIG. 3. SAGE calculation using a 550 μm inner diameter ring with the small (left) and large (right) backlighter targets.

FIG. 5. Cutaway of a Saturn ring used for these experiments with actual (nominal) dimensions in mm.

FIG. 7. From top: nuclear yield, ion temperature (T_i), average D^{3}He proton energy (E_p) and Gaussian width (σ), and nuclear bang time. For yield and T_i, both DD and D^{3}He data are shown.

2 μm thick SiO_2 walls produced via the drop tower technique, and filled with 6 atm of D_2 and 12 atm of ^{3}He gas. The capsules are driven with eight NIF quads from the 44.5° cones (12T, 22T, 32T, 45T, 14B, 25B, 35B, and 43B) using a 900 ps duration square pulse with a peak power of 2.2 TW/beam and a total drive energy of 51 kJ. Relative to previously reported NIF backlighter results from Rygg *et al.*,[22] this drive is more energetic (6 → 8 quads) but more representative of the configurations used in radiography physics experiments on the NIF.

Top-level nuclear data from these experiments are shown in Fig. 7, compared to the shot reported in Ref. 22 (N150325-001). The data shown, from the top of the figure, are the nuclear yield and ion temperature (T_i) for both DD and D^{3}He fusion, average D^{3}He proton energy (E_p) and Gaussian width (σ), and nuclear bang time. DD neutron data (yield and T_i) are measured using the neutron time of flight (NTOF) detectors,[33] the D^{3}He proton spectra are measured using Wedge Range Filter (WRF) spectrometers[34] and the Magnetic Recoil Spectrometer (MRS),[35,36] and the nuclear bang time is measured using the proton Time of Flight (PTOF) detector.[37] Several proton spectrometers are fielded at various locations around the target chamber on a shot. The WRFs are mounted to DIMs using a bracket that places the spectrometers at ±13° in θ and ±3° in ϕ. The MRS is in a fixed location at $\theta = 73°$, $\phi = 324°$. The values shown in Fig. 7 represent a weighted mean across all available diagnostics on a given shot. The MRS measurements typically have the smallest uncertainty and thus have the greatest weight.

We observe that the smaller capsule implosions, both with and without the Saturn ring, have lower nuclear yields (by about $5 - 10\times$), higher energy D^{3}He proton energies (by ~400 keV), and earlier bang times (by ~500 ps). The shots have similar ion temperature and spectral width. The lower yield can largely be explained by
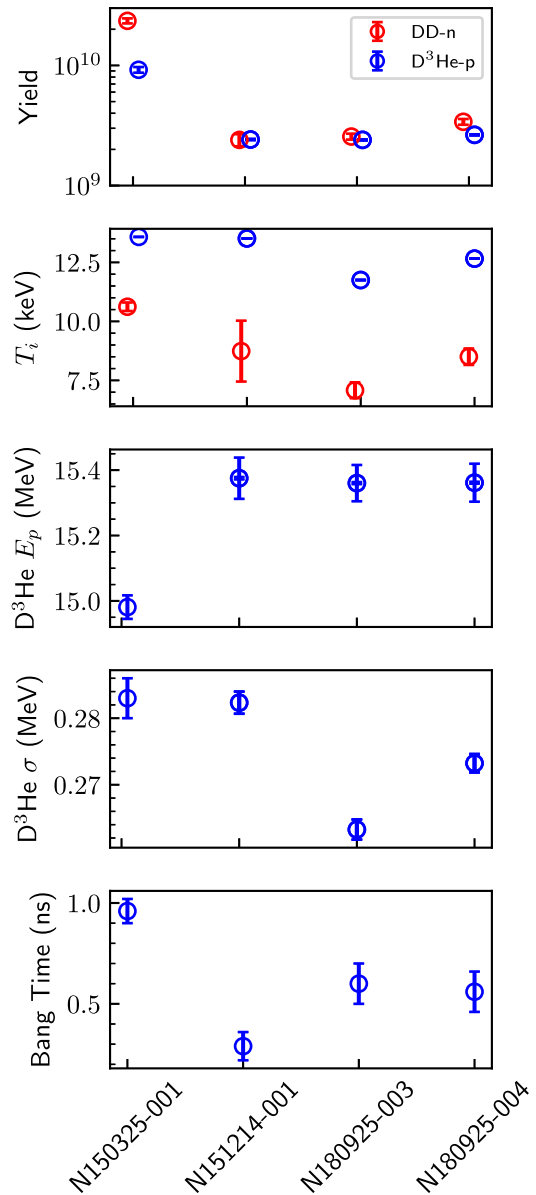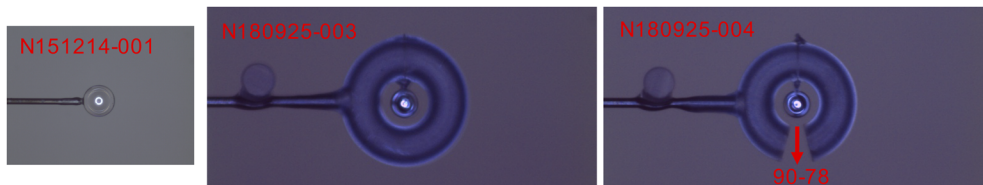

FIG. 6. Targets used for the shots in this study: no Saturn ring (N151214-001), a full ring (N180925-003), and a ring with a 30° cutaway toward DIM 90-78 (N180925-004).

the smaller fuel volume with the smaller capsules. The higher proton energy is expected since the nuclear bang time for the smaller capsules occurs earlier during the peak of the laser irradiation when electric charging of the capsule is strong.[39–41]

As discussed in Ref. 22, the source isotropy is an important characteristic for radiography applications. Figure 8 shows the D^3He proton data [mean energy (left), yield (center), and spectral width (σ, right)] for the three small-capsule shots in this study [N151214-001 (top), N180925-003 (center), and N180925-004 (bottom)]. For each shot and quantity, the data are shown by the detector's location in target-chamber coordinates (θ, ϕ). The proton spectral width is consistent among all detectors. The yield is isotropic with the exception of the detectors near DIM 90-78 ($\theta = 76°–103°$ and $\phi \sim 78°$) on shot N180925-004, which will be discussed in further detail later in this section.

The proton energy is upshifted from the birth energy [see Eq. (2)] by several hundred keV. There is a clearly apparent anisotropy where the polar detectors are upshifted by 200 keV–300 keV more than the equatorial detectors. This is further illustrated in Fig. 9, which shows the proton spectra measured on each shot. The polar detectors, at $\theta = 13°$, are shown in blue and orange and are clearly at higher energy than the equatorial detectors on N180925-003 and N180925-004, especially when comparing to the high-quality data from the MRS at (73, 324).

Several other features are notable in the spectra. First, we observe an occasional low-energy tail on the proton spectra for the

equatorial WRF detectors for the shots with Saturn rings. The WRFs are displaced from the equatorial plane by only ±13°, which is similar to the maximum extent of the ring (also ±13°) at the highest point. However, some protons may undergo large-angle Coulomb scattering from the ring into the detector line of sight, or ablated material from the ring may enter the line of sight, creating such a tail. This suggests that, in applications, care must be taken that data near the ring are sufficiently separated to avoid interference from scattered or downshifted protons. It is notable that the MRS spectra, taken 17° from the equator and not obstructed by the ring, do not show a low-energy tail.

It is immediately apparent that the detectors near DIM 90-78 on shot N180925-004 have substantially suppressed proton yield (red and green curves with spectra near zero protons/MeV). This is surprising, since the 30° cutout is oriented in this direction, and those detectors should have a clear view of the imploded backlighter capsule. Figure 10 shows the measured proton yield vs detector angle (θ, ϕ) for shot N180925-004. In addition to the WRF and MRS data, Fig. 10 includes the yield measured using a penumbral imaging configuration in the DIM.[42,43] It is clear that the effective proton fluence measured near the cutout is suppressed by a factor of $\gtrsim 20\times$ compared to the other detectors. Since the proton energy is not largely impacted (see Fig. 9), the low fluence must result from an orthogonal electromagnetic field deflecting the protons, which presumably originates from the cutout. Based on this result, we conclude that a cutout ring is not viable for charged-particle measurements in
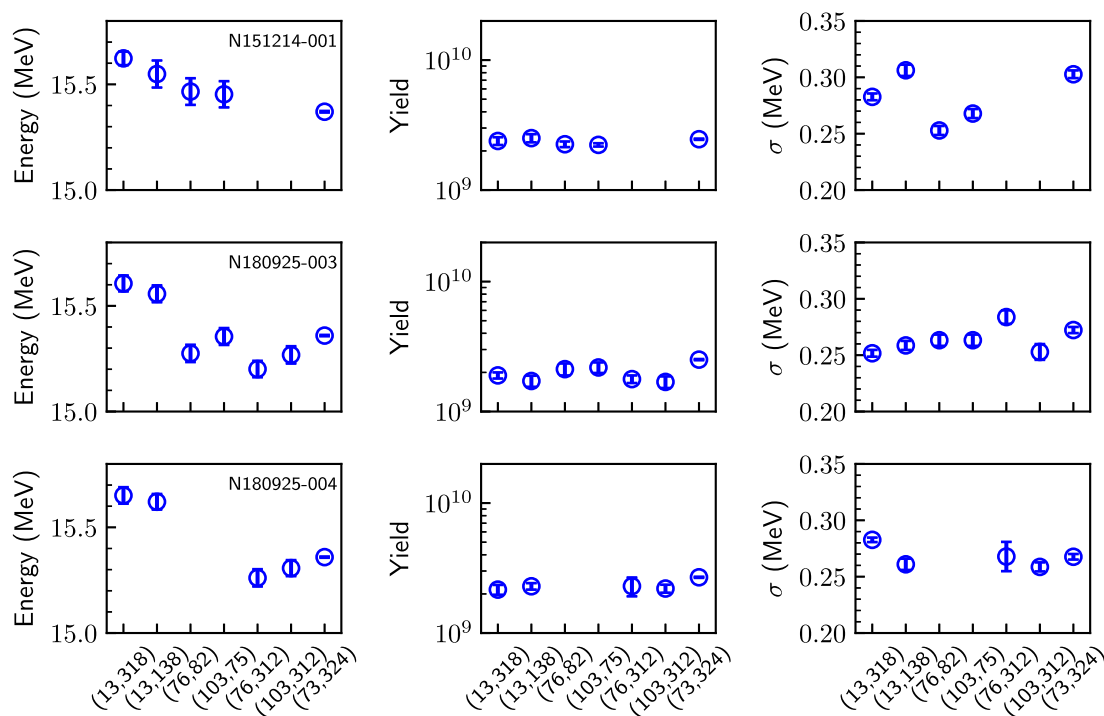

FIG. 8. D^3He proton energy (left), yield (center), and width (σ, right) for the three shots in this study: N151214-001 (no ring, top), N180925-003 (full ring, center), and N180925-004 (cutout ring, bottom). Data are shown vs detector location in target-chamber coordinates (θ, ϕ).
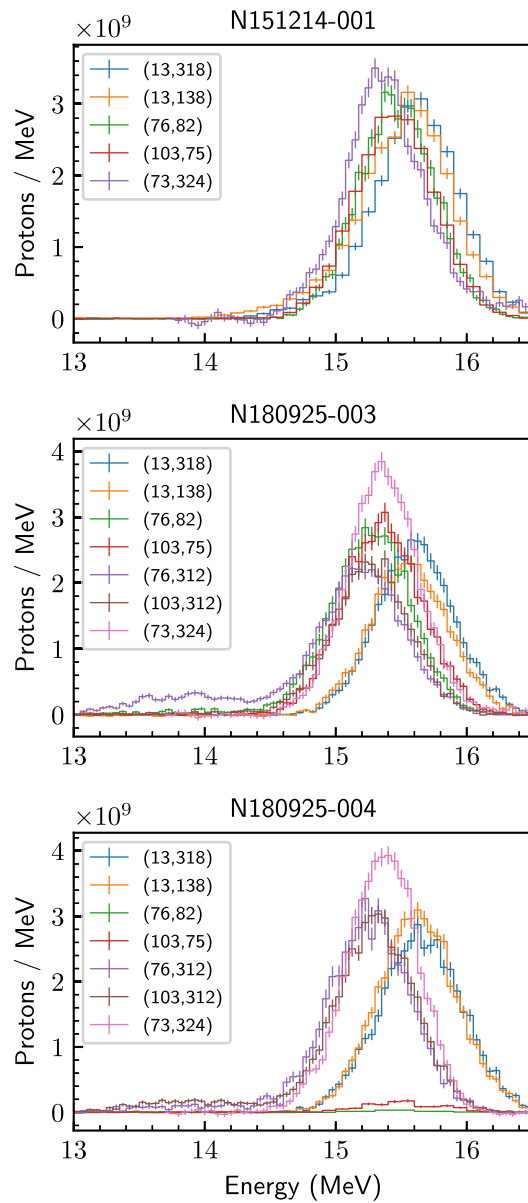
FIG. 9. Measured proton spectra by various WRFs and the MRS [located at (73, 324)], labeled by location in target-chamber coordinates (θ, ϕ).

FIG. 10. Measured D^{3}He proton yield vs detector location (θ, ϕ) for shot N180925-004, with the cutout ring. Detectors near the cutout are shown in red, including the two WRFs [(76,82) and (103,75)] plus the data point at (90,78) from the penumbral imaging detector in the DIM.

TABLE I. Measured proton source size (P_0), quoted in terms of the full-width at half-maximum (FWHM) for the three shots with 440 μm capsules.

Shot	P_0 (μm)
N151214-001	57.1 ± 3.4
N180925-003	60.0 ± 2.5
N180925-004	62.5 ± 2.5

the plane of the ring. Given that the field strength is sufficient to deflect 15 MeV protons by a substantial angle, this configuration may have interesting applications as a generation mechanism for intense electromagnetic fields.

The last critically important metric for backlighter performance is the proton source size, which typically dominates the effective imaging resolution. The source size is measured using proton penumbral imaging in the polar DIM.[42,43] Unlike Ref. 22, which showe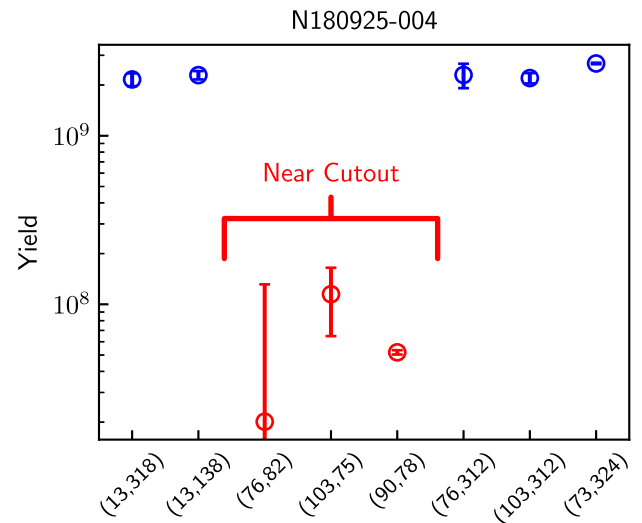d proton emission images, we are only able to report source sizes rather than images due to the lower yield of these smaller capsules, and because a DIM alignment error caused partial loss of the penumbra on the Saturn ring shots. The results are given in Table I. The three shots are consistent with a full-width at half-maximum (FWHM) source size ~60 μm, which is ~20 μm smaller than the source size reported by Rygg *et al.* for the larger capsules.[22] Typical radiography applications use object distances on the order of 1 cm resulting in several thousand protons per resolution element even with the reduced yields for small capsules; proton fluence contrast in typical radiography experiments (e.g., Refs. 19 and 20) is often 2× or better so particle statistics are a negligible contribution to the resolution, which is still dominated by the source size.

IV. CONCLUSION

In summary, we report on a demonstration of "Saturn" targets as a proton backlighter for radiography experiments on the NIF. Electromagnetic fields in high-energy-density plasmas are often diagnosed with charged-particle deflectometry; capsule implosions using DD and D^{3}He fuel to generate fusion protons are

commonly used as a backlighter. On the NIF, relatively large capsules (860 μm diameter) have been typically used,[22] in part due to concerns over damage risks to the laser system due to unabsorbed laser light when using smaller capsules, since the focus spot size of the NIF phase plates is much larger than the capsules. In this work, we report the development of "Saturn" targets using smaller capsules (440 μm diameter) in which a ring is placed around the equator of the capsule to block any blow-by light and increase flexibility in experimental configurations. The performance of small capsule implosions is unaffected by the presence of a ring. We test an equatorial cutout in the ring as a potential route toward measurements in the plane of the ring but find that large electromagnetic fields around the cutout render this approach infeasible. For applications, especially use as a proton backlighter, measurement axes near the ring plane are not viable, but above ~15° from the ring plane is feasible.

The fusion source size of these small capsules is significantly reduced compared to previous results,[22] with unabsorbed laser light mitigated by the ring. The small capsules produce lower nuclear yields, which is expected due to the reduced volume; this must be considered depending on the application. In summary, these results offer a route toward proton radiography using fusion sources with improved spatial resolution on the NIF.

ACKNOWLEDGMENTS

DATA AVAILABILITY

Raw data were generated at the NIF. The data that support the findings of this study are available from the corresponding author upon reasonable request.

REFERENCES

[1] A. Schlüter and L. Biermann, Z. Nat. A **5**, 237–251 (1950).

[2] J. A. Stamper, K. Papadopoulos, R. N. Sudan, S. O. Dean, E. A. McLean, and J. M. Dawson, Phys. Rev. Lett. **26**, 1012–1015 (1971).

[3] G. Fiksel, A. Agliata, D. Barnak, G. Brent, P.-Y. Chang, L. Folnsbee, G. Gates, D. Hasset, D. Lonobile, J. Magoon, D. Mastrosimone, M. J. Shoup III, and R. Betti, Rev. Sci. Instrum. **86**, 016105 (2015).

[4] J. A. Cobble, R. P. Johnson, T. E. Cowan, N. Renard-Le Galloudec, and M. Allen, J. Appl. Phys. **92**, 1775–1779 (2002).

[5] M. Borghesi, D. H. Campbell, A. Schiavi, M. G. Haines, O. Willi, A. J. MacKinnon, P. Patel, L. A. Gizzi, M. Galimberti, R. J. Clarke, F. Pegoraro, H. Ruhl, and S. Bulanov, Phys. Plasmas **9**, 2214–2220 (2002).

[6] A. J. Mackinnon, P. K. Patel, R. P. Town, M. J. Edwards, T. Phillips, S. C. Lerner, D. W. Price, D. Hicks, M. H. Key, S. Hatchett, S. C. Wilks, M. Borghesi, L. Romagnani, S. Kar, T. Toncian, G. Pretzler, O. Willi, M. Koenig, E. Martinolli, S. Lepape, A. Benuzzi-Mounaix, P. Audebert, J. C. Gauthier, J. King, R. Snavely, R. R. Freeman, and T. Boehlly, Rev. Sci. Instrum. **75**, 3531–3536 (2004).

[7] A. B. Borghesi, C. K. Li, H. G. Rinderknecht, F. H. Séguin, R. D. Petrasso, C. Stoeckl, D. D. Meyerhofer, P. Nilson, T. C. Sangster, S. Le Pape, A. Mackinnon, and P. Patel, Rev. Sci. Instrum. **83**, 013511 (2012).

[8] C. K. Li, F. H. Séguin, J. A. Frenje, J. R. Rygg, R. D. Petrasso, R. P. J. Town, P. A. Amendt, S. P. Hatchett, O. L. Landen, A. J. Mackinnon, P. K. Patel, V. A. Smalyuk, J. P. Knauer, T. C. Sangster, and C. Stoeckl, Rev. Sci. Instrum. **77**, 10E725 (2006).

[9] M. J.-E. Manuel, A. B. Zylstra, H. G. Rinderknecht, D. T. Casey, M. J. Rosenberg, N. Sinenian, C. K. Li, J. A. Frenje, F. H. Séguin, and R. D. Petrasso, Rev. Sci. Instrum. **83**, 063506 (2012).

[10] A. J. Mackinnon, P. K. Patel, M. Borghesi, R. C. Clarke, R. R. Freeman, H. Habara, S. P. Hatchett, D. Hey, D. G. Hicks, S. Kar, M. H. Key, J. A. King, K. Lancaster, D. Neely, A. Nikkro, P. A. Norreys, M. M. Notley, T. W. Phillips, L. Romagnani, R. A. Snavely, R. B. Stephens, and R. P. J. Town, Phys. Rev. Lett. **97**, 045001 (2006).

[11] J. R. Rygg, F. H. Séguin, C. K. Li, J. A. Frenje, M. J.-E. Manuel, R. D. Petrasso, R. Betti, J. A. Delettrez, O. V. Gotchev, J. P. Knauer, D. D. Meyerhofer, F. J. Marshall, C. Stoeckl, and W. Theobald, Science **319**, 1223–1225 (2008).

[12] C. K. Li, F. H. Séguin, J. A. Frenje, R. D. Petrasso, P. A. Amendt, R. P. J. Town, O. L. Landen, J. R. Rygg, R. Betti, J. P. Knauer, D. D. Meyerhofer, J. M. Soures, C. A. Back, J. D. Kilkenny, and A. Nikroo, Phys. Rev. Lett. **102**, 205001 (2009).

[13] C. K. Li, F. H. Séguin, J. A. Frenje, M. Rosenberg, R. D. Petrasso, P. A. Amendt, J. A. Koch, O. L. Landen, H. S. Park, H. F. Robey, R. P. J. Town, A. Casner, F. Philippe, R. Betti, J. P. Knauer, D. D. Meyerhofer, C. A. Back, J. D. Kilkenny, and A. Nikroo, Science **327**, 1231–1235 (2010).

[14] G. Fiksel, W. Fox, A. Bhattacharjee, D. H. Barnak, P.-Y. Chang, K. Germaschewski, S. X. Hu, and P. M. Nilson, Phys. Rev. Lett. **113**, 105003 (2014).

[15] M. J. Rosenberg, C. K. Li, W. Fox, A. B. Zylstra, C. Stoeckl, F. H. Séguin, J. A. Frenje, and R. D. Petrasso, Phys. Rev. Lett. **114**, 205004 (2015).

[16] M. J. Rosenberg, C. K. Li, W. Fox, I. Igumenshchev, F. H. Séguin, R. P. J. Town, J. A. Frenje, C. Stoeckl, V. Glebov, and R. D. Petrasso, Nat. Commun. **6**, 6190 (2015).

[17] L. Gao, P. M. Nilson, I. V. Igumenschev, S. X. Hu, J. R. Davies, C. Stoeckl, M. G. Haines, D. H. Froula, R. Betti, and D. D. Meyerhofer, Phys. Rev. Lett. **109**, 115001 (2012).

[18] M. J.-E. Manuel, C. K. Li, F. H. Séguin, J. Frenje, D. T. Casey, R. D. Petrasso, S. X. Hu, R. Betti, J. D. Hager, D. D. Meyerhofer, and V. A. Smalyuk, Phys. Rev. Lett. **108**, 255006 (2012).

[19] C. M. Huntington, F. Fiuza, J. S. Ross, A. B. Zylstra, R. P. Drake, D. H. Froula, G. Gregori, N. L. Kugland, C. C. Kuranz, M. C. Levy, C. K. Li, J. Meinecke, T. Morita, R. Petrasso, C. Plechaty, B. A. Remington, D. D. Ryutov, Y. Sakawa, A. Spitkovsky, H. Takabe, and H.-S. Park, Nat. Phys. **11**, 173–176 (2015).

[20] C. K. Li, P. Tzeferacos, D. Lamb, G. Gregori, P. A. Norreys, M. J. Rosenberg, R. K. Follett, D. H. Froula, M. Koenig, F. H. Seguin, J. A. Frenje, H. G. Rinderknecht, H. Sio, A. B. Zylstra, R. D. Petrasso, P. A. Amendt, H. S. Park, B. A. Remington, D. D. Ryutov, S. C. Wilks, R. Betti, A. Frank, S. X. Hu, T. C. Sangster, P. Hartigan, R. P. Drake, C. C. Kuranz, S. V. Lebedev, and N. C. Woolsey, Nat. Commun. **7**, 13081 (2016).

[21] P. Tzeferacos, A. Rigby, A. F. A. Bott, A. R. Bell, R. Bingham, A. Casner, F. Cattaneo, E. M. Churazov, J. Emig, F. Fiuza, C. B. Forest, J. Foster, C. Graziani, J. Katz, M. Koenig, C.-K. Li, J. Meinecke, R. Petrasso, H.-S. Park, J. S. Remington, B. A. Ross, D. Ryu, D. Ryutov, T. G. White, B. Reville, F. Miniati, A. A. Schekochihin, D. Q. Lamb, D. H. Froula, and G. Gregori, Nat. Commun. **9**, 1–8 (2018).

[22] J. R. Rygg, A. B. Zylstra, F. H. Séguin, S. LePape, B. Bachmann, R. S. Craxton, E. M. Garcia, Y. Z. Kong, M. Gatu-Johnson, S. F. Khan, B. J. Lahmann, P. W. McKenty, R. D. Petrasso, H. G. Rinderknecht, M. J. Rosenberg, D. B. Sayre, and H. W. Sio, Rev. Sci. Instrum. **86**, 116104 (2015).

[23] C.-K. Li, private communication (2015).

[24] M. L. Spaeth, K. R. Manes, D. H. Kalantar, P. E. Miller, J. E. Heebner, E. S. Bliss, D. R. Spec, T. G. Parham, P. K. Whitman, P. J. Wegner, P. A. Baisden, J. A. Menapace, M. W. Bowers, S. J. Cohen, T. I. Suratwala, J. M. Di Nicola, M. A. Newton, J. J. Adams, J. B. Trenholme, R. G. Finucane, R. E. Bonanno, D. C. Rardin, P. A. Arnold, S. N. Dixit, G. V. Erbert, A. C. Erlandson, J. E. Fair, E. Feigenbaum, W. H. Gourdin, R. A. Hawley, J. Honig, R. K. House, K. S. Jancaitis, K. N. LaFortune, D. W. Larson, B. J. Le Galloudec, J. D. Lindl, B. J. MacGowan, C. D. Marshall, K. P. McCandless, R. W. McCracken, R. C. Montesanti, E. I. Moses, M. C. Nostrand, J. A. Pryatel, V. S. Roberts, S. B. Rodriguez, A. W. Rowe, R. A. Sacks, J. T. Salmon, M. J. Shaw, S. Sommer, C. J. Stolz, G. L. Tietbohl, C. C. Widmayer, and R. Zacharias, Fusion Sci. Technol. **69**, 25–145 (2016).

[25] S. Le Pape, private communication (2017).

[26] R. S. Craxton, F. J. Marshall, M. J. Bonino, R. Epstein, P. W. McKenty, S. Skupsky, J. A. Delettrez, I. V. Igumenshchev, D. W. Jacobs-Perkins, J. P. Knauer, J. A. Marozas, P. B. Radha, and W. Seka, Phys. Plasmas **12**, 056304 (2005).

[27] F. J. Marshall, R. S. Craxton, M. J. Bonino, R. Epstein, V. Y. Glebov, D. Jacobs-Perkins, J. P. Knauer, J. A. Marozas, P. W. McKenty, S. G. Noyes, P. B. Radha, W. Seka, S. Skupsky, and V. A. Smalyuk, J. Phys. IV **133**, 153–157 (2006).

[28] R. S. Craxton and D. W. Jacobs-Perkins, Phys. Rev. Lett. **94**, 095002 (2005).

[29] R. S. Craxton and R. L. McCrory, J. Appl. Phys. **56**, 108–117 (1984).

[30] L. Browning, Development of a standardized Saturn ring for proton backlighting on the National Ignition Facility, Laboratory for Laser Energetics, 2016, Summer Research Program for High School Juniors.

[31] B. J. MacGowan, private communication (2015).

[32] R. Zhang, private communication (2015).

[33] V. Y. Glebov, T. C. Sangster, C. Stoeckl, J. P. Knauer, W. Theobald, K. L. Marshall, M. J. Shoup, T. Buczek, M. Cruz, T. Duffy, M. Romanofsky, M. Fox, A. Pruyne, M. J. Moran, R. A. Lerche, J. McNaney, J. D. Kilkenny, M. J. Eckart, D. Schneider, D. Munro, W. Stoeffl, R. Zacharias, J. J. Haslam, T. Clancy, M. Yeoman, D. Warwas, C. J. Horsfield, J.-L. Bourgade, O. Landoas, L. Disdier, G. A. Chandler, and R. J. Leeper, Rev. Sci. Instrum. **81**, 10D325 (2010).

[34] A. B. Zylstra, J. A. Frenje, F. H. Séguin, M. J. Rosenberg, H. G. Rinderknecht, M. G. Johnson, D. T. Casey, N. Sinenian, M. J.-E. Manuel, C. J. Waugh, H. W. Sio, C. K. Li, R. D. Petrasso, S. Friedrich, K. Knittel, R. Bionta, M. McKernan, D. Callahan, G. W. Collins, E. Dewald, T. Döppner, M. J. Edwards, S. Glenzer, D. G. Hicks, O. L. Landen, R. London, A. Mackinnon, N. Meezan, R. R. Prasad, J. Ralph, M. Richardson, J. R. Rygg, S. Sepke, S. Weber, R. Zacharias, E. Moses, J. Kilkenny, A. Nikroo, T. C. Sangster, V. Glebov, C. Stoeckl, R. Olson, R. J. Leeper, J. Kline, G. Kyrala, and D. Wilson, Rev. Sci. Instrum. **83**, 10D901 (2012).

[35] M. G. Johnson, J. A. Frenje, D. T. Casey, C. K. Li, F. H. Séguin, R. Petrasso, R. Ashabranner, R. M. Bionta, D. L. Bleuel, E. J. Bond, J. A. Caggiano, A. Carpenter, C. J. Cerjan, T. J. Clancy, T. Doeppner, M. J. Eckart, M. J. Edwards, S. Friedrich, S. H. Glenzer, S. W. Haan, E. P. Hartouni, R. Hatarik, S. P. Hatchett, O. S. Jones, G. Kyrala, S. Le Pape, R. A. Lerche, O. L. Landen, T. Ma, A. J. MacKinnon, M. A. McKernan, M. J. Moran, E. Moses, D. H. Munro, J. McNaney, H. S. Park, J. Ralph, B. Remington, J. R. Rygg, S. M. Sepke, V. Smalyuk, B. Spears, P. T. Springer, C. B. Yeamans, M. Farrell, D. Jasion, J. D. Kilkenny, A. Nikroo, R. Paguio, J. P. Knauer, V. Yu Glebov, T. C. Sangster, R. Betti, C. Stoeckl, J. Magoon, M. J. Shoup, G. P. Grim, J. Kline, G. L. Morgan, T. J. Murphy, R. J. Leeper, C. L. Ruiz, G. W. Cooper, and A. J. Nelson, Rev. Sci. Instrum. **83**, 10D308 (2012).

[36] D. T. Casey, J. A. Frenje, M. Gatu Johnson, F. H. Séguin, C. K. Li, R. D. Petrasso, V. Y. Glebov, J. Katz, J. P. Knauer, D. D. Meyerhofer, T. C. Sangster, R. M. Bionta, D. L. Bleuel, T. Döppner, S. Glenzer, E. Hartouni, S. P. Hatchett, S. Le Pape, T. Ma, A. MacKinnon, M. A. Mckernan, M. Moran, E. Moses, H.-S. Park, J. Ralph, B. A. Remington, V. Smalyuk, C. B. Yeamans, J. Kline, G. Kyrala, G. A. Chandler, R. J. Leeper, C. L. Ruiz, G. W. Cooper, A. J. Nelson, K. Fletcher, J. Kilkenny, M. Farrell, D. Jasion, and R. Paguio, Rev. Sci. Instrum. **83**, 10D912 (2012).

[37] H. G. Rinderknecht, M. G. Johnson, A. B. Zylstra, N. Sinenian, M. J. Rosenberg, J. A. Frenje, C. J. Waugh, C. K. Li, F. H. Sèguin, R. D. Petrasso, J. R. Rygg, J. R. Kimbrough, A. MacPhee, G. W. Collins, D. Hicks, A. Mackinnon, P. Bell, R. Bionta, T. Clancy, R. Zacharias, T. Döppner, H. S. Park, S. LePape, O. Landen, N. Meezan, E. I. Moses, V. U. Glebov, C. Stoeckl, T. C. Sangster, R. Olson, J. Kline, and J. Kilkenny, Rev. Sci. Instrum. **83**, 10D902 (2012).

[38] W. J. Hibbard, M. D. Landon, M. D. Vergino, F. D. Lee, and J. A. Chael, Rev. Sci. Instrum. **72**, 530–532 (2001).

[39] M. J.-E. Manuel, N. Sinenian, F. H. Séguin, C. K. Li, J. A. Frenje, H. G. Rinderknecht, D. T. Casey, A. B. Zylstra, R. D. Petrasso, and F. N. Beg, Appl. Phys. Lett. **100**, 203505 (2012).

[40] N. Sinenian, A. B. Zylstra, M. J.-E. Manuel, H. G. Rinderknecht, J. A. Frenje, F. H. Séguin, C. K. Li, R. D. Petrasso, V. Goncharov, J. Delettrez, I. V. Igumenshchev, D. H. Froula, C. Stoeckl, T. C. Sangster, D. D. Meyerhofer, J. A. Cobble, and D. G. Hicks, Appl. Phys. Lett. **101**, 114102 (2012).

[41] N. Sinenian, M. J.-E. Manuel, J. A. Frenje, F. H. Séguin, C. K. Li, and R. D. Petrasso, Plasma Phys. Controlled Fusion **55**, 045001 (2013).

[42] F. H. Séguin, J. L. DeCiantis, J. A. Frenje, S. Kurebayashi, C. K. Li, J. R. Rygg, C. Chen, V. Berube, B. E. Schwartz, R. D. Petrasso, V. A. Smalyuk, F. J. Marshall, J. P. Knauer, J. A. Delettrez, P. W. McKenty, D. D. Meyerhofer, S. Roberts, T. C. Sangster, K. Mikaelian, and H. S. Park, Rev. Sci. Instrum. **75**, 3520–3525 (2004).

[43] A. B. Zylstra, H.-S. Park, J. S. Ross, F. Fiuza, J. A. Frenje, D. P. Higginson, C. Huntington, C. K. Li, R. D. Petrasso, B. Pollock, B. Remington, H. G. Rinderknecht, D. Ryutov, F. H. Séguin, D. Turnbull, and S. C. Wilks, Rev. Sci. Instrum. **87**, 11E704 (2016).